Journal of Aeronautical
-Science and Engineering-, Vol.2

May 20, 2015

Computational Fluid Dynamic Studies On Helicopter Main-Rotor-Hub Assembly Unsteady Wake

I.S. Ishak,[a,*], Shuhaimi Mansor, [b], Tholudin Mat Lazim,[c]

Department of Aeronatical, Automotive and Ocean Engineering, Faculty of Mechanical Engineering Universiti Teknologi Malaysia, 81310 UTM Skudai, Johor, Malaysia
[a)]shah@mail.fkm.utm.my, [b)]shuhaimi@mail.fkm.utm.my, [c)]tholudin@fkm.utm.my

*Corresponding author: shah@mail.fkm.utm.my

Paper History

Received: 10-Apr-2015
Received in revised form: 20-Apr-2015
Accepted: 19-May-2015

ABSTRACT

The helicopter tail shake phenomenon is an area of great concern to helicopter manufacturers as it adversely affects the overall performance and handling qualities of the helicopter, and the comfort of its occupants. This study aims to gain information of the flow field that governs helicopter tail shake phenomenon which has frequently puzzled the aerodynamicists. Using Computational Fluid Dynamic (CFD) approach, the Multiple Reference Frames (MRF) method was applied to simulate the helicopter's main-rotor-hub assembly rotation. In this study, the aerodynamic flow field was computed using the Reynolds-Averaged Navier-Stokes (RANS) equations. As the induced wake, which consequently causing tail to shake differs with the rpm of main-rotor-hub assembly, this preliminary numerical investigation was performed ranging from rpm of 0 to 900, with intervals of 300 rpm. A rotor-hub-fairing which covers partly the main-rotor-hub assembly was also employed to examine its effect on the wake unsteadiness. Results tell the rotation of main-rotor-hub assembly and pylon do significantly influencing the flow unsteadiness.

KEY WORDS: *Flow Field; Helicopter Tail Shake; Unsteady Flow; Computational Fluid Dynamic.*

NOMENCLATURE

CFD	Computational Fluid Dynamic
FFT	Fast-Fourier Transform
GAMBIT	Geometry And Mesh Building Intelligent Toolkit
LES	Large Eddy Simulation
MRF	Multiple Reference Frames
PSD	Power Spectral Density
RANS	Reynolds-Averaged Navier-Stokes
RPM	Rotation Per Minute
UTM-LST	Universiti Teknologi Malaysia - Low Speed Tunnel

1.0 INTRODUCTION

Tail shake is an issue of major concern for rotorcraft [1] as it is adversely affected the overall performance and handling qualities of helicopter. Vibrations transmitted from vertical tail to cockpit have also caused discomfort to the occupants [2]. It had being reported on the AH-64D Longbow Apache helicopter, the vibration resulted had increased the cockpit lateral vibration levels, which consequently increased crew workload and reduced their ability to perform precision tasks [3].

This phenomenon is a challenging issue to understand with as it involves an interaction between aerodynamic flow excitation, which related to flight parameters and structural response, which related to structure characteristics [2]. A good understanding of this matter is necessary as a typical aspect of tail shake that it has unsteady random character, indicating that the wake induced excitation is in also unsteady of nature [2].

Tail shake phenomenon happens partly due to the unsteady flow contributed from the main-rotor-hub assembly that hit the tail part, as shown in Figure 1.

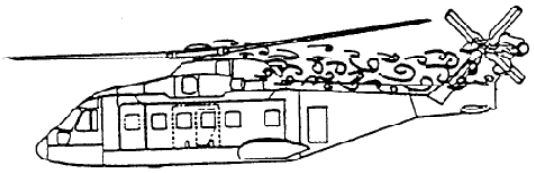

Figure 1: Schematic diagram of tail shake [2]

Hence, this phenomenon is likely only to happen when there is a forward velocity i.e. helicopter is unlikely to encounter this tail shake problem during hovering or vertical climb/descent,. In this research, focus will be on main-rotor-hub assembly's wake as it is believed to be the major contributor of the problem. This allows the tail shake investigation to be conducted using blade-stubs configuration [4,5,6]. Blade-stubs configuration is a combination of main-rotor-hub assembly but with shorter rotor blades.

2.0 METHODOLOGY

This numerical study used **R**eynolds-**A**veraged **N**avier-**S**tokes (**RANS**) equation models which solve ensemble-averaged Navier-Stokes equations [7]. The two-equation models of Realizable k-ε model were employed in this numerical modelling where the **M**ultiple **R**eference **F**rames (MRF) approach was applied to simulate the main-rotor-hub-assembly rotation at various rpm.

This numerical investigation used an ellipsoidal fuselage [8] with the axes ratio of longitudinal to lateral axes is 4.485. This kind of model is selected as it avoids geometric complexity and simplifies the interactions with the wake [8]. For this research work, the longitudinal axes were taken as 1120 mm. The model is shown in Figure 2.

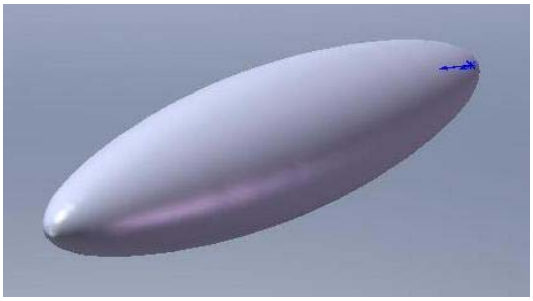

Figure 2: An ellipsoidal fuselage [8]

The model is equipped with a simplified main-rotor-hub assembly attached with shorter blades i.e. blade-stubs configuration, as shown in Figure 3. This simplified main rotor hub assembly is meant to trigger the unsteady wake due to rotation of main- rotor-hub assembly.

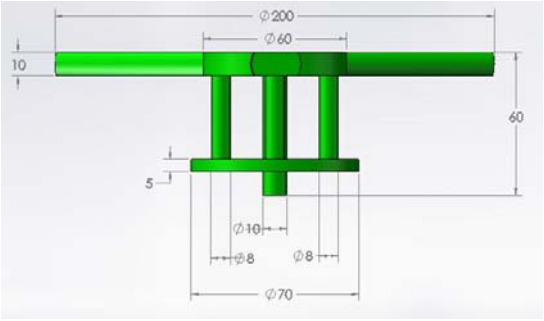

Figure 3: A simplified blade-stubs configuration (unit in millimetre)

Figure 4 depicts the complete model with blade-stubs configuration mated with an ellipsoidal pylon.

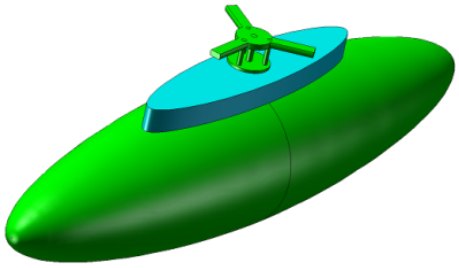

Figure 4: Model for CFD simulation

In **G**eometry **A**nd **M**esh **B**uilding **I**ntelligent **T**oolkit (**GAMBIT**), which acts as a pre-processor for CFD analysis, a test section with a size of 2m (width) x 1.5m (height) x 5.8m (length) was virtually created for placing the model. The size of this test section is similar as the test section size of Universiti Teknologi Malaysia – Low Speed Tunnel (UTM-LST), as experimental works are also be planned to compare with this CFD analysis.

In MRF method, two reference frames must be created with one at the vicinity of the rotating parts i.e. main-rotor-hub assembly. As there is no specific rule regarding the size of the frame for rotating parts, this research decided to take the distance of the frame's boundary to surface of the rotating parts to be 1 aerofoil thickness. The aerofoil thickness of the main rotor, as depicted in Figure 3, is 10 mm and hence the frame was created in such manner as shown in Figure 5.

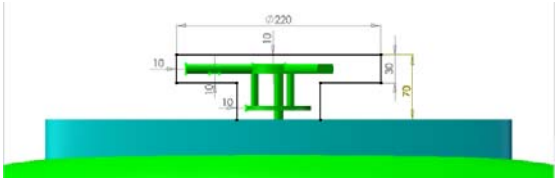

Figure 5 (a): Frame dimensions (unit in millimetre)

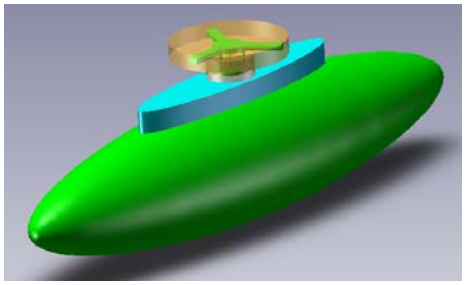

Figure 5(b): Frame for rotating parts

Figure 5: Frame for rotating parts

3.0 RESULTS AND DISCUSSION

Before running the final simulation, independence grid analysis had been carried out to verify the results obtained are free from grid influence. This is important to confirm the differences of results are due to test configurations, not due to number of the grid.

All simulation results presented throughout this paper were run at wind speed, or forward flight velocity, of 40 m/s and at zero angle of attack.

Figures 6 and 7 show the path lines of turbulent intensity for 0 and 900 rpm of main-rotor-hub assembly, respectively.

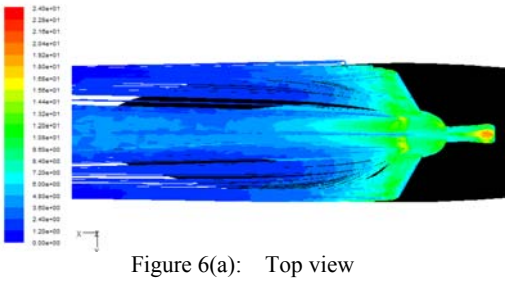

Figure 6(a): Top view

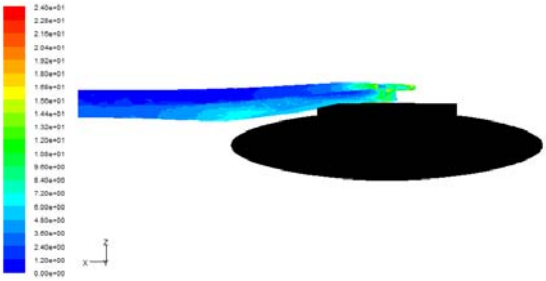

Figure 6(b): Side view

Figure 6: Path line of turbulent intensity (%) at 0 rpm

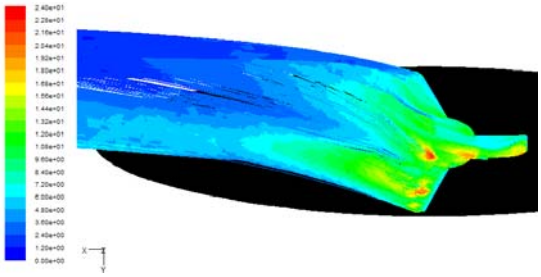

Figure 7(a): Top view

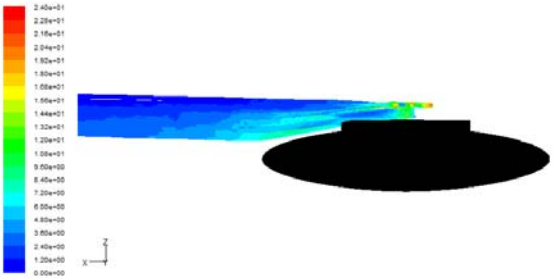

Figure 7(b): Side view

Figure 7: Path lines of turbulent intensity (%) at 900 rpm

Viewed from top as shown by Figures 6(a) and 7(a), the path lines are about symmetrical on both left and right sides for 0 rpm, contrary for 900 rpm, the path lines are unsymmetrical indicating there is strong flow interaction with the rotating main-rotor-hub assembly.

Compared to Figure 6(b), turbulent intensity is higher and wake volume is thicker in Figure 7(b). This shows rotation on main-rotor-hub assembly triggers a significant unsteady wake which could contribute to tail shake problem.

Figures 8 and 9 depict the flow unsteadiness at the vicinity of vertical tail i.e. 'vertical-tail-plane' for 0 and 900 main-rotor-hub assembly rpm, respectively.

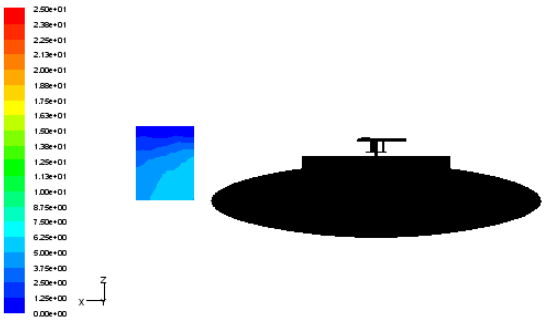

Figure 8: Contours of turbulent intensity (%) at 0 rpm

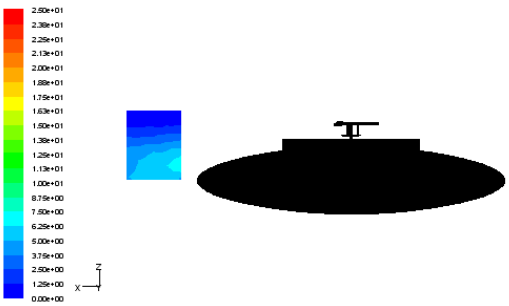

Figure 9: Contours of turbulent intensity (%) at 900 rpm

Obviously it can be noticed at 900 rpm, there is more flow unsteadiness compared to at 0 rpm. This justifies the rotor blade rotation does influencing the flow unsteadiness.

Table 1 depicts the values of turbulent intensity in this 'vertical-tail-plane', ranging from 0 to 900 rpm with intervals of 300 rpm.

Table 1: Turbulent intensity (%)

Main Rotor Rpm	Turbulent Intensity (%) Facet max.
0	6.54
300	6.69
600	6.90
900	7.15

It indicates main-rotor-hub assembly rpm increases the turbulent intensity in which is tally with the results of experimental work using a 14% scaled-down generic model of Eurocopter 350Z helicopter done by Ishak et al. [9].

Figure 10 shows total pressure contours for different main-rotor-hub assembly rpm as pressure fluctuations could be translated into aerodynamic forces excitation which may lead to tail vibration.

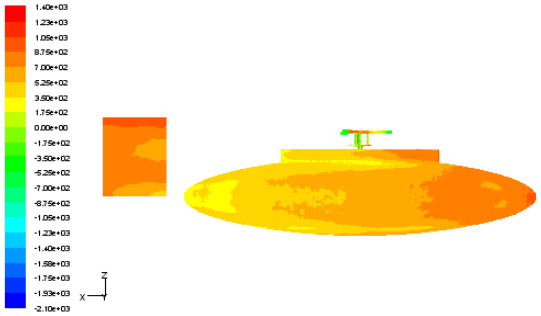

Figure 10(a): 0 rpm

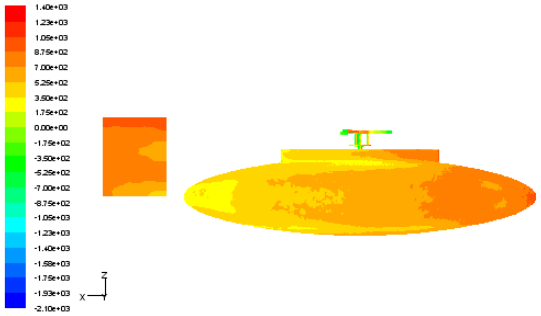

Figure 10(b): 300 rpm

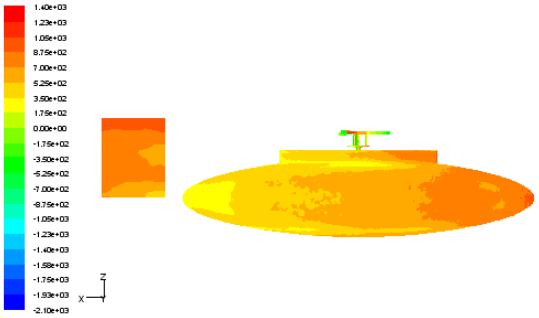

Figure 10 (c): 600 rpm

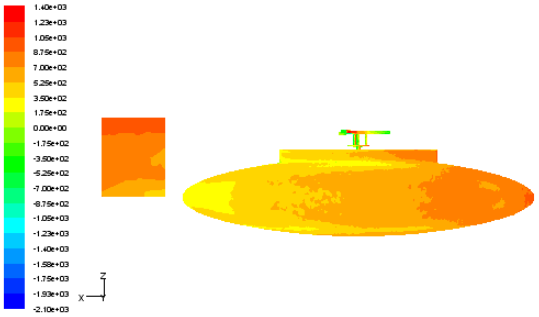

Figure 10 (d): 900 rpm

Figure 10: Contours of total pressure (Pa)

The figures depict the fluctuation of total pressure inside the 'vertical-tail-plane' is becoming more with the increment of main-rotor-hub assembly rpm. Table 2 summarizes the maximum and minimum values of total pressure inside this 'vertical-tail-plane'.

Table 2: Total pressure (Pa)

Main Rotor Rpm	Total Pressure (Pa)		ΔFacet (Pa)
	Facet max.	Facet min.	
0	940.24	349.16	591.08
300	940.67	337.17	603.50
600	941.11	324.48	616.63
900	943.08	318.36	624.72

The table indicates the range from minimum to maximum value of total pressure i.e. Δ Facet, is getting larger with the increment of main-rotor-hub assembly rpm. This result translates more aerodynamic forces excitation occurred with higher rotation of main-rotor-hub assembly, signaling could mean more tail shake problem.

To investigate the effects of covering some parts of main-rotor-hub assembly, pylon height is increased i.e. acting as a rotor-hub-fairing, as shown in Figure 11.

Fuselage *Pylon height be increased*

Figure 11: Model configuration with fairing attached

Figures 12 and 13 show path lines with fairing configuration.

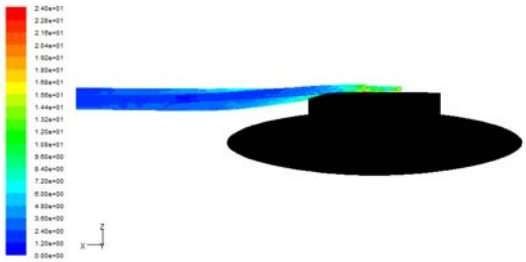

Figure 12: Path lines colored by turbulent intensity (%) from 'main-rotor-hub assembly' at 0 rpm

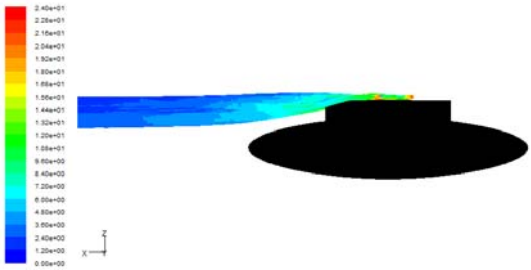

Figure 13: Path lines colored by turbulent intensity (%) from 'main-rotor-hub assembly' at 900 rpm

The path lines demonstrated by Figures 12 and 13 behave the same trend as with configuration without fairing i.e. more turbulent intensity and wake volume at 900 rpm compares to at 0 rpm configuration.

Compares to Figure 7, Figure 13 translates with fairing configuration, the unsteady wake is reduced both in term of the wake's unsteadiness and volume.

Figure 14 shows total pressure contours for different rpm of main-rotor-hub assembly with fairing configuration.

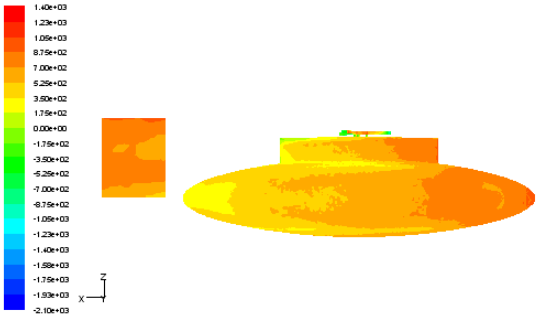

Figure 14(a): 0 rpm

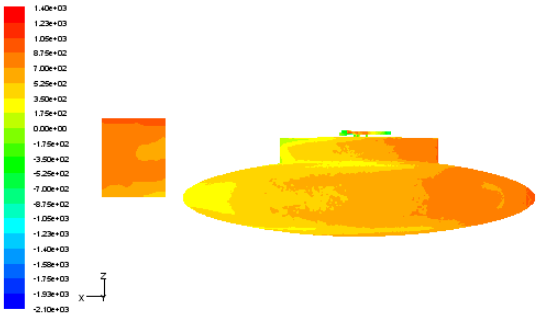

Figure 14(b): 300 rpm

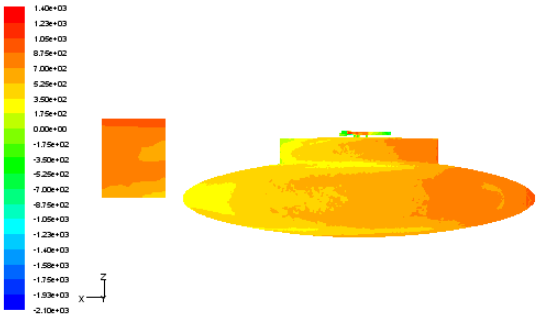

Figure 14(c): 600 rpm

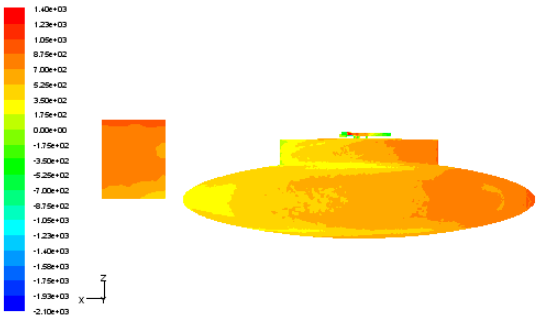

Figure 14(d): 900 rpm

Figure 14: Contours of total pressure (Pa)

Same as depicted by Figure 10 for configuration without fairing, the figures narrate higher pressure fluctuation occurred at higher rotation of main-rotor-hub assembly.

Table 3 shows the maximum and minimum values of total pressure inside the vicinity of vertical plane with fairing configuration.

Table 3:Total pressure (with fairing configuration)

Main rotor rpm	Total Pressure (Pa)		ΔFacet (Pa)
	Facet max.	Facet min.	
0	936.37	356.93	579.44
300	938.12	351.54	586.58
600	937.99	348.02	589.97
900	937.41	338.21	599.20

Table 3 concludes the same trend as in Table 2 i.e. ΔFacet increases with the rpm of main-rotor-hub assembly. However its value is smaller compared to Table 2, which interprets lesser aerodynamic excitation happens that might be translated to a lesser tail shake problem.

An investigation was also being carried out trying to correlate the flow unsteadiness with aerodynamic drag, as shown by Figure 15.

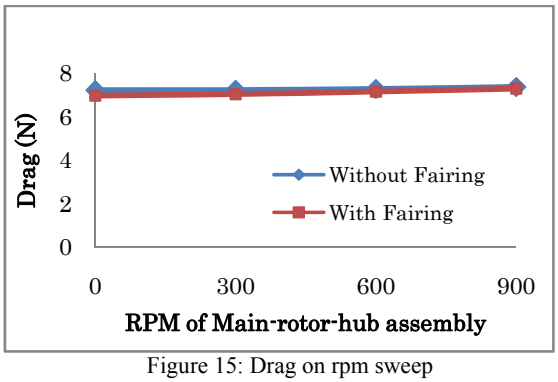

Figure 15: Drag on rpm sweep

Figure 15 reveals there is correlation between aerodynamic drag with main-rotor-hub assembly rotation i.e. the aerodynamic drag is increased, even though merely increment, with the incremental of main-rotor-hub assembly rpm. Referred back to Tables 1 and 2 which show main-rotor-hub assembly rpm increases flow unsteadiness, it seems correlation could be made between flow unsteadiness with aerodynamic drag in which higher flow unsteadiness seems generating more aerodynamic drag. This correlation is found agreeable with the results of experimental work done by Ishak et al. [9].

Figure 15 also depicts configuration with fairing is better in term of generating lesser aerodynamic drag. As depicted previously by Figure 14 and Table 3 that fairing leads to lesser flow unsteadiness, this result seems agreeable with the correlation made that flow unsteadiness could influence aerodynamic drag.

4.0 EXPERIMENTAL WORKS

In order to verify the simulation findings, experimental works were conducted in the Universiti Teknologi Malaysia's low-speed closed-return wind tunnel (UTM-LST) as shown in Figure 16. The test section is 2.0m (W) x 1.5m (H) x 5.8m (L) with the maximum test wind speed of 80 ms^{-1}.

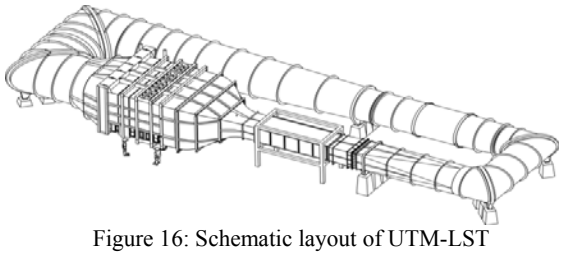

Figure 16: Schematic layout of UTM-LST

4.1 Test Configurations

Figure 17 depicts the diagrams for No Fairing Configuration and With Fairing Configuration for the experimental works.

(a) No Fairing Configuration

(b) With Fairing Configuration

Figure 17: Wind tunnel test configurations

It is noted the physical shapes of main-rotor-hub assembly and the fairing are not exactly as the same as those in the simulation works, but this research is keen more on the results' trends rather than their absolute values.

The total pressure distribution and its rms value are the main interest of this work as the pressure fluctuations could be translated into wake unsteadiness in the term of aerodynamic forces excitation that may lead to tail vibration.

With the aid of wake rake housing KULITE miniature dynamic pressure transducers type XCL-072-10PSID, the mapping of total pressure was conducted at the downstream of main-rotor-hub assembly. Figure 18 illustrates the schematic diagram of this experimental work and Figure 19 shows the testing be conducted, respectively.

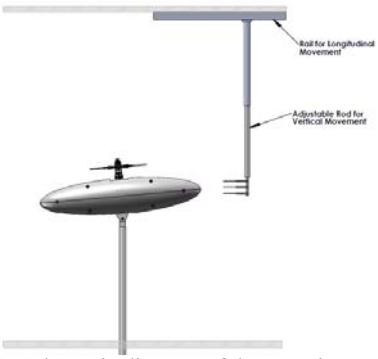

Figure 18: Schematic diagram of the experiment

Figure 19: Experimental works at UTM-LST

However as the scope of this paper is stressed on the simulation works, only one point of investigation shown in Figure 20 will be analysed for the verification on the findings from simulation works.

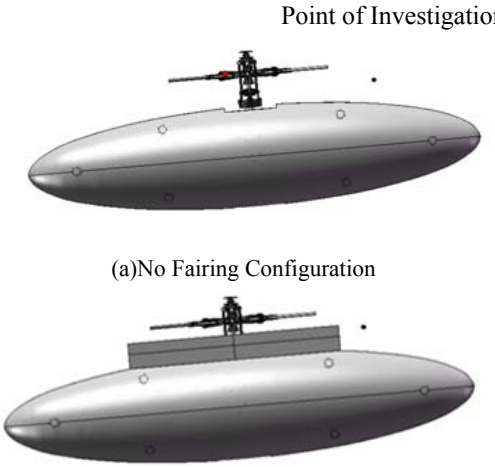

(a)No Fairing Configuration

(b) With Fairing Configuration

Figure 20: Schematic diagram for the research point location (the single dotted point)

The sampling rate and number of samples for this experimental works are chosen to be 5kHz and 300 000 data, respectively. This choice is made after previous study finds these data sampling parameters are appropriate for implementing the dynamic analysis.

4.2 Power Spectral Density (PSD) Analysis

Power spectral density (PSD) describes how the power of a signal or time series is distributed with frequency. For this research work, it was done directly by the method called Fast-Fourier Transform (FFT) in which enabling the studies on frequencies and their respective amplitudes.

Analyses done reveal with fairing mated to the main-rotor-hub assembly, there were 69.29% energy reduction of total pressure (Pa^2/Hz) and 44.59% reduction on total pressure fluctuations (RMS value). These results coincide and thus verify the numerical findings that conclude fairing does help reducing the wake unsteadiness.

5.0 CONCLUSION

This research works serve as a preliminary numerical study on helicopter tail shake phenomenon. Yet using a very simplified model, this research has successfully gives some initial predictions of the flow field that governs the helicopter tail shake phenomenon where the results' trends are in a good agreement with the results of experimental works done by Ishak et al. [9].

Results tell main-rotor-hub assembly's rpm influences the flow unsteadiness i.e. at higher rotation, higher turbulent intensity and bigger pressure fluctuations be triggered. This higher aerodynamic excitation likely will contribute to higher helicopter's tail vibration.

Adding fairing seems will reduce aerodynamic drag, as well the wake's unsteadiness. This finding could mean a lesser tail shake problem if some of the rotating parts of main-rotor-hub assembly being covered.

Nevertheless, more comprehensive simulation works should be done at various configurations for better comprehensive conclusions. On top of that, **L**arge **E**ddy **S**imulation (**LES**) coupled with Sliding Mesh Method, are much required for a better understanding of this helicopter tail shake phenomenon.

ACKNOWLEDGEMENTS

Authors would like to thank Abd Basid Abd Rahman, Mohd Riza Abdul Rahman, Airi Ali and Muhammad Khaidhir Jamil, from Universiti Teknologi Malaysia, for their assistance during this research implementation.

REFERENCE

1. F.N. Coton (2009). *Evaluation Report of UTM Research Project*, University of Glasgow.
2. P.G. de Waad and M. Trouvé (1999). *Tail shake vibration,* National Aerospace Laboratory (NLR), American Helicopter Society Annual Forum,.
3. A. Hassan, T. Thompson, E.P.N. Duque, and J. Melton (1999). *Resolution of tail buffet phenomena for AH-64D™ Longbow Apache™*, Journal American Helicopter Society,

Volume 44.

4. A. Cassier, R. Weneckers and J-M Pouradier (1994). *Aerodynamic development of the tiger helicopter*, 50th American Helicopter Society Forum.
5. C. Hermans et al. (1997). *The NH90 helicopter development wind tunnel programme*, European Aerospace Societies Conference, Cambridge UK.
6. *Eurocopter Slide Presentation* (2006), France.
7. *Introductory FLUENT Notes* (2005), FLUENT V6.2.
8. P.F. Lorber, T.A. Egofl (1988). *An Unsteady Helicopter Rotor-Fuselage Interaction Analysis*, NASA Contractor Report 4178.
9. I.S. Ishak, S. Mansor, T. Mat Lazim (2008). *Experimental Research On Helicopter Tail Shake Phenomenon*, Issue 26, Jurnal Mekanikal, Universiti Teknologi Malaysia.